CHAPTER 3

CHARACTERIZATION OF COCOA NIBS, PREPARED ACTIVATED CARBON AND DEASH ACTIVATED CARBON

3.1 Introduction

Agricultural by-products and its wastes offer cheap and abundant source of activated carbons. These materials have less or none economic importance but the responsible authorities face the disposal problem. The conversion of agricultural waste into activated carbons would offer significant economic value to the community, overcome the waste disposal issues and above all offer an inexpensive alternative to the common precursor of commercially available activated carbons (Demirbas, 2009). Commercial activated carbons usually prepared from precursors for instance coal, wood and peat which are non-renewable and relatively high in cost (Yahya et al., 2015).

Afterwards, activated carbon could be derived from all lignocellulosic material. Although the carbon contents in agricultural waste are relatively low compared to coal, wood and peat, but the costs involve give a considerably significant influence for its selection. Low carbon contents yield low activated carbon but with its high volatile matters, agricultural waste are suitable to be used as precursor in producing an extremely porous adsorbent (Yahya et al., 2015).

Ash content, pyrolysis and activation process are among the critical factors that can affect the quality of the prepared activated carbon. It is a challenge to produce highly surface area activated carbon when ash content is high (Schröder et al., 2011).

The preparation of activated carbon involves two basic processes: physical activation and chemical activation. In the physical activation process, the precursor is carbonized first into char. Then the char is activated with an oxidizing agent such as carbon dioxide or steam. In the chemical activation process, the precursor is impregnated with a chemical activating agent. Then the impregnated precursor is carbonized at different temperatures (Okman et al., 2014). The chemical activation process has advantages compared with physical activation, where the activation can be achieved at lower carbonization temperature and in lesser time of activation. Besides, chemical activation produces mesoporous activated carbon with a larger surface area (Sahira et al., 2013).

Usually, the activating agent used are basic salts and bases. The chemicals that are frequently used are zinc chloride ($ZnCl_2$), phosphoric acid (H_3PO_4), potassium hydroxide (KOH) and sodium hydroxide (NaOH). Among these chemical, KOH and NaOH are corrosive, and hazardous while $ZnCl_2$ has issue on environmental disadvantages other than being corrosive reagent (Adinata et al., 2007). H_3PO_4 is a corrosive acid, can form toxic fumes when in contact with organic compounds and usually used in non-food products (Singleton, 2015).

A more nonthreatening chemical is preferred as activating agent in preparing the medicinal grade activated carbon. Therefore, potassium carbonate (K_2CO_3) is chosen as it not a hazardous chemical and not harmful as it is commonly used in food products (Adinata et al., 2007). Impregnation with K_2CO_3 is a simple process but offers a highly porous carbon structure (Hamza et al., 2016).

Ash in an activated carbon is an impurity or residue in the carbonaceous material. Ash is consisting of minerals such as silica (Si), aluminum (Al), iron (Fe), magnesium (Mg) and calcium (Ca). Certain minerals could seep into the liquid matrix

from the activated carbon during the applications. It will compete for the adsorption sites with adsorbates during the adsorption process (Ahmad et al., 2013b). The ash fills and blocks the existing pores that results in a decrease in the surface area (Rafiq et al., 2016).

Ash can be removed or reduced from inhibiting the pores in activated carbon using demineralization process (López et al., 2013). Demineralization process involves the dissolution of minerals and metals into acid or alkali solutions such as hydrochloric acid (HCl), nitric acid (HNO_3), sulfuric acid (H_2SO_4) or NaOH (Manocha et al., 2013). Ahmad et al. (2013b) named the process as de-ash treatment, where HCl was used to dissolve the minerals.

There was a massive amount of characterization and adsorption data made available from adsorption experiments. There was also numerous variables to characterize the activated carbon prepared in these studies such as surface area, total pore volume, micropore and mesopore volumes, pore size distribution, surface chemistry, surface morphology and elemental composition (Ahmad et al., 2013b; Purnomo et al., 2012; Guo et al., 2009). However, the most important is to extract the useful information from the data to correlate their influence with the adsorbent performance in adsorption (Á'lvarez-Uriarte et al., 2011).

In order to extract these data and gather that information, statistical instrument is usually applied. One way to approach data reduction and formal interpretation is by using principal component analysis (PCA). PCA is used to reduce the dimensionality of a data set having a large number of interrelated variables and can be used as a discriminant technique (Bartel et al., 2013). PCA explores the common variance and extracts significant factors or components from the data ('Alvarez-Uriarte et al., 2011).

In this study, PCA was applied to correlate the patterns, groups and trends in the characterization data. By using PCA, more precise evaluation of the influence of each property on the characteristics can be established. The studied variables were surface area, mesopore volume, pore size and surface functional groups. Overall, seventeen activated carbon samples were compared.

Thus, the objectives of this chapter were to determine the characterization of the precursor used, to prepare and characterize the prepared activated carbon from cocoa nib pellet, to determine the effect of demineralization process onto the prepared activated carbon and to identify the main variables, out of a set of 13 variables, which consist of structural, physical, and chemical properties of the activated carbons that mostly effect the adsorption performance using PCA.

3.2 Materials

The carbonaceous precursor used for preparation of activated carbon is cocoa nib pellets were supplied by the Cocoa Innovative and Technology Centre (CITC), Malaysian Cocoa Board, Nilai, Negeri Sembilan. Commercial activated carbons were procured from Merck, Germany (Ultracarbon Medicinal Charcoal) and Cabot (Norit Activated Charcoal). All chemical reagents used in this work were procured from the Merck, Malaysia (hydrochloric acid 30%), Fisher Scientific, Malaysia (nitric acid 67 %), Essex, UK (sodium hydroxide 99 %) and Systerm (potassium carbonate 99.5 %).

3.3 Methods

3.3.1 Proximate Analysis of the Precursor

Proximate analysis of the cocoa nibs was carried out by using a muffle furnace method (moisture and ash contents) (Ahmad et al., 2011). The moisture and ash content determination was performed using crucible with cover which was pre-dried prior use. Approximately, 2 g of sample was weighed into the crucible and was placed into the pre-heated furnace (Nabertherm B180, Germany) at 104 ^{0}C for one hour (moisture content) and at 600 °C for 12 hours (ash content).

The equations to calculate the moisture and ash contents are as in equation 3.1 and 3.2, respectively:

(3.1) Moisture, M (%) $= \frac{W-B}{W}$ x 100

where W is the weight of sample used (g) and B is the weight of sample after drying (g) in moisture test.

(3.2) Ash, A (%) $= \frac{F-G}{W}$ x 100

where F is the weight of crucible and ash residue (g) and G is the weight of empty crucible.

3.3.2 Ultimate Analysis of the Precursor

For elemental analysis, approximately 100 mg of samples was weighed into tin boats of CHNS analyzer (Elementar vario MACRO Cube, Germany). Each sample was analyzed twice. The carbon (C), hydrogen (H), nitrogen (N) and sulphur (S) content and the difference in element concentration between the two measurements (repeatability) are recorded (Elementar, 2017).

Heavy metal analysis was conducted by an Inductively Coupled Plasma Mass Spectrometer (Agilent 7500 Series, USA). Prior analysis, solid samples were digested into liquid using microwave digestion. Approximately, 0.1 mg of sample was weighed and transferred into a digestion vessel. About 1.5 mL HNO_3 was added to each vessel. The sample was prepared in triplicate. Three blanks were included in each analytical batch.

3.3.3 Surface Morphology

Scanning electron microscope (SEM - FEI Quanta 450, US) was used to study the surface morphology of the precursors, chars and the activated carbon prepared including the pore structure, surface structure and pore arrangement. Coating is a must for a non-conductive specimen (Fei, 2003). According to Dufek & Hayles (2003), coating was applied to increase stability of the beam and to improve the image quality.

The sample (cocoa nibs) was coated evenly with 1 to 5 nm layer of Palladium at all direction. The coated sample was mounted onto the sample chamber with a sample holder. The instrument function settings were adjusted to compliment the analysis. The image was obtained by using imaging procedures, where the high voltage was ramped. The appeared image was focused, adjusted and corrected in order to capture the high-resolution image (Pathan et al., 2010).

3.3.4 Surface Chemistry

Fourier transform infrared (Agilent 630 FTIR, US) spectroscopy was conducted to study the surface chemistry of the precursors, chars and the prepared activated carbons by identifying the functional groups presented on the samples. Various infrared

light wavelengths was measured for the sample and recorded using a suitable method (Higgins & Seelebinder, 2011).

Prior analysis, the background spectrum was collected. Then approximately, 0.05 g of sample was placed onto the crystal plate. The sample was put in contact with the attached FTIR device by turn down the knob until a 'click' sound was heard. Then the sample was analyzed and the created spectrum was saved for data handling.

3.3.5 Principal Component Analysis

The relationship between variables on characteristics of the prepared activated carbons and the commercial activated carbons were explained using principal component analysis (PCA), a common tool in multivariate analysis (Al-Degs et al., 2012). By conducting various porosity and surface chemistry experiments, the similarities between the prepared activated carbons and the commercial activated carbons were studied.

Initially, the data collected from surface area, porosity and surface chemistry experiments were subjected for PCA to evaluate the impact of the studied variables between two groups of activated carbons (the prepared and the commercial activated carbons). In PCA, the data matrix, X is consists of variable, k and objects, n (Jolliffe & Cadima, 2016). The variables were surface area, pore volume, pore diameter and surface chemistry (in peaks of chemical groups) while the objects were the prepared activated carbons and the commercial activetd carbons. The study was performed by translating the variables into loadings and the objects into scores vectors (Al-Degs et al., 2012).

PCA was carried out using Unscrambler software (X10) from Camo, USA. Two new matrices: principal component scores (P) and principal component loadings (W)

were developed during the experiment. The matrix P describes the relationship between the objects and matrix W clarifies the relationship between the variables. The significant principal component factors were plotted (P1 vs P2) for analysis purposes. The data is composed of a matrix X of dimension 17 × 11.

3.3.6 Experimental Setup

The experimental setup for the preparation of the activated carbon is shown in Figure 3.1. It involved two main parts:

a. Gas metering section to control the gas flow rate as required (Dwyer, US).
b. Stainless steel vertical tubular furnace coupled with programmable temperature controller (Carbolite VST 12/110/900, United Kingdom).

Nitrogen (N_2) gas was supplied to the system at constant pressure which was adjusted using pressure regulators and the flow rate was determined by gas flow meters. The gas stream was passed to the back side of the vertical furnace and connected to the reactor from the lower end of the tubular furnace. The Teflon tubing joined by stainless steel fittings was assembled as the connecting pipe for the system.

The process of pyrolysis, carbonization and activation of the precursor and char were accomplished in a stainless steel vertical furnace. The furnace is comprises of a fixed bed reactor, a vertical tubular electric furnace, a temperature controller (Linn Elektro Therm, Germany), flow meters and a ventilation exhaust. The size of the vertical reactor is 100 cm length and 6.9 cm width of 310 grade stainless steel.

The reactor was placed at central position in the vertical tubular furnace. The system was attached with a temperature controller and a Type-K (chromel alumel) thermocouple to control and monitor the temperature. The furnace can tolerate to a maximum tolerant temperature of 1200 °C. The smoke emitted from the reactor was

condensed in water condenser at the bottom of the system through condenser tubing. The schematic diagrams of the experimental setup used in this study are shown in Figure 3.1.

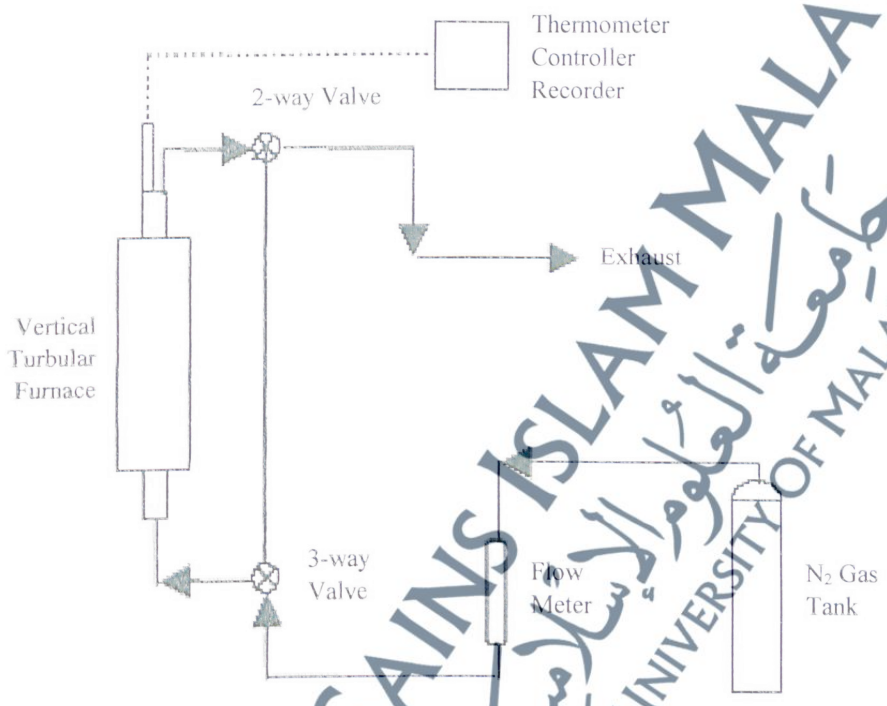

Figure 3.1 Schematic diagram of the experimental setup in preparing activated carbon.

3.3.7 Carbonization

About 60 g of precursor was weighed and transferred into a furnace equipped with stainless steel vertical tubular reactor. Nitrogen gas was used as the purging gas through the furnace, to inhibit oxidization from happen. The flow rate of nitrogen gas was set at 1.5 mL/min and the heating rate was held constant at 10 °C/min. The temperature was ramped from room temperature to 700 °C and held for one hour. After the one-hour holding time, the temperature was decreased to 30 °C to collect the produced char. The char was kept in desiccator to cool down to room temperature and

maintaining the moisture content. The char was then stored in air-tight container for further treatment (Ahmad et al., 2011).

Calculation of the char yield is as in equation 3.4:

$$\text{Yield (\%)} = \frac{W_C}{W_i} \times 100 \quad (3.4)$$

where W_c is the mass of char (g) after carbonization process and W_i is the initial mass of cocoa nib pellet before carbonization.

3.3.8 Potassium Carbonate Impregnation

The chars produced were impregnated with potassium carbonate (K_2CO_3) at various impregnation ratios (IR) as in Table 3.1. The K_2CO_3 pellets and the char were mixed together with hot deionized water in a 250 mL beaker. The mixture was stirred and then the beakers were immersed in water bath shaker at constant temperature and speed rate. The mixing was performed at 30 °C for three hours at 100 rpm to make sure that the K_2CO_3 pellets were completely dissolved. Then, the beaker was placed inside an oven for overnight at temperature 105 °C for dehydrating purpose, leaving only K_2CO_3 on the sample (Adinata et al., 2007).

The impregnation ratio was calculated as in equation 3.5:

$$IR = \frac{W_{K_2CO_3}}{W_{char}} \times 100 \quad (3.5)$$

where $W_{K_2CO_3}$ is the dry weight (g) of potassium carbonate pellets and W_{char} is the dry weight (g) of char.

Table 3.1 The impregnation ratio (IR) on K_2CO_3 and char

IR	K_2CO_3 (g)	Char (g)
1:1	20	20
2:1	40	20
3:1	60	20

3.3.9 Pyrolysis

The K_2CO_3-impregnated chars were placed inside the vertical tubular furnace reactor for activation under nitrogen flow of 150 cm^3/min. The temperature was ramped from ambient temperature (25 °C) to desired activation temperature (500, 600, 700 and 800 °C) at heating rate of 10 °C/min. Once the desired activation temperature was reached, the temperature was held for one hour. The activated carbons were cooled to room temperature under nitrogen flow (Ahmad et al., 2014). Table 3.2 shows the activation temperature applied for the activated carbon.

Table 3.2 The activation temperature applied for each IR

Activation	IR	Temperature (°C)
1	1:1	500
2	2:1	500
3	3:1	500
4	1:1	600
5	2:1	600
6	3:1	600
7	1:1	700
8	2:1	700
9	3:1	700
10	1:1	800
11	2:1	800
12	3:1	800

3.3.10 Washing

The activated carbons produced were washed with hot deionized water to recover the remaining K_2CO_3. The washing process was continued using hydrochloric acid (0.1 M), then washed several times with hot deionized water until the pH of the washing solutions reached 6-7. The pH was measured using pH meter. Filter paper and filter funnel were used in the washing process. The washed activated carbons were then kept in an oven at 105 °C until the activated carbons were totally dried. The dried activated carbons prepared were stored in air-tight containers for further characterization and adsorption studies (Ahmad et al., 2011).

Once the activated carbon was prepared, characterization process was performed to determine its characteristics. The characterizations study include surface area and porosity measurement, surface morphology determination and surface functional group identification.

3.3.11 Surface Area and Porosity Measurement

The surface area, pore volume and pore size distribution of the prepared activated carbons were determined from the adsorption isotherms of nitrogen at 77 K (-196.15 °C) onto the samples. The surface area and porosity analyzer (Micromeritics ASAP 2020, USA) operated by measuring the quantity of gas absorbed onto a solid surface at equilibrium vapor pressure by the static volumetric method.

A quartz sample tube was used to contain the analyzed sample. A cleaned quartz sample tube was weighed together with frit seal on an analytical balance and the weight was recorded. Approximately 1.0 gram of the sample (in crushed and fine particles) was added into the tube and weighed together with the frit seal and the weight was also recorded. The quartz sample tube was connected with degas port with connector nut,

ferrule and *O*-ring (frit seal was not removed). Degassing evacuates moisture and volatiles contained in the tube. A heating mantle was clipped the bulb of the tube with a mantle clip. Then the samples were degassed from ambient temperature to 300 °C until evacuation was completed at 950 mmHg. After the degas procedure completed, the sample was transferred to the analysis system where it was cooled in liquid nitrogen. A 21-points analysis was carried out at -196.15 °C to obtain the nitrogen adsorption-desorption isotherm by admitting successive known volumes of nitrogen in and out of the sample and measuring the equilibrium pressure (Micromeritics, 2011).

A relative pressure of between 10^{-5} and 0.995 of N_2 gas and 10^{-9} was used to obtain the N_2 adsorption isotherm. The calculations of surface area, pore volume and average pore size were performed by the software (Micropore version 2.46). The surface area and total pore volume of the activated carbons were calculated from the N_2 adsorption isotherms using the Brunauer-Emmett-Teller (BET), Langmuir and Barrett, Joyner and Halenda (BJH) equations (Ahmad et al., 2012) meanwhile the micropore volume has been calculated by applying Horvath–Kawazoe (HK) method (Orkun et al., 2012).

3.3.12 Demineralization of the Activated Carbon

In order to remove the ash residue, acid leaching process was performed. This process used hydrochloric acid to treat the prepared activated carbon. The acid treatment on the activated carbon was also called demineralization (Manocha et al., 2013).

Approximately, 10g of prepared activated carbon was added into 250 mL beaker which contained 1M of HCl. A continuous but controlled heat was supplied to the mixture using a magnetic stirrer with heating ceramic plate. The temperature controller was adjusted to maintain a constant temperature (50 °C) for one hour. A thermometer

was placed in the beaker to monitor the temperature in real-time. After finished, the washing procedure was applied (Ahmad et al., 2011).

Similarly, the demineralized (or de-ash) activated carbons were characterized for its physical and chemical characterizations: surface area and porosity, surface morphology and surface functional groups.

3.4 Results and Discussion

3.4.1 Characterization of the Precursor

3.4.1.1 Proximate Analysis

Table 3.3 shows the proximate analysis between two precursors: cocoa nibs and cocoa shells. The comparisons were made to study the differences between the two precursors. The differences were addressed in the ash content, moisture content, fat content and the pH value.

Percentage of moisture content in cocoa nibs was significantly higher (9.62 %) compared with cocoa shell (8.37 %). However, the ash content was considerably lower in cocoa nibs (6.08 %) compared with cocoa shell (8.63 %). The percentage yield of cocoa shells (32.75 %) was significantly higher compared with cocoa nibs (28.07).

Table 3.3 Comparison on proximate analysis of cocoa nibs and cocoa shells

Precursor	Moisture (%)	Ash (%)	% Yield	Reference
Cocoa nib	9.62	6.08	28.07	Present work
Cocoa shell	8.37	8.63	30.75	(Ahmad et al., 2013b)

Both moisture contents were relatively higher (8.37 – 9.62 %) compared with the acceptable limit (6 – 7 %) for long term storage of cocoa. The moisture content of the cocoa should be fairly reduced after the cocoa beans undergone the fermentation process. However, fermentation itself is believed to introduce the moisture to the beans (Afoakwa et al., 2011).

Aprotosoaie et al. (2016) reported that the ash content in cocoa nibs was in the range of 2.3 % to 3.5 % for fermented and unfermented cocoa nibs. Adeyeye (2015) reported that the ash content in fat-free cocoa nibs was 6.0 %, where evidently similar to our findings (6.08 %).

Minerals such as potassium (K), magnesium (Mg), phosphorus (P), calcium (Ca), copper (Cu), zink (Zn), sodium (Na) and iron (Fe) are usually presence in cocoa nibs (Afoakwa et al., 2011). The ash content is a determination of the total amount of minerals present within a food. Precursor with fairly large proportion of mineral matter results in higher ash yields on air dried basis (Saini et al., 2015). However, the content would be differed due to several factors.

Pod storage and fermentation process are among factors that could affect the content of minerals in cocoa nibs (Afoakwa et al., 2011). The pH of the soil could has influence the uptake of minerals and availability of nutrients to the cocoa trees. Various nutrients and minerals could be unavailable when acidity is increase, and some minerals could present excessively which can lead to toxicity (van Vliet et al, 2015).

3.4.1.2 Ultimate Analysis

Table 3.4 shows the percentage of the major elements in cocoa nibs namely carbon, hydrogen, nitrogen and sulphur. The cocoa nibs contained high carbon (C)

content (44.56 %) and relatively low content of sulphur (S) (0.26 %). The percentage of nitrogen (N) and hydrogen (H) were 4.23 % and 7.20 %, respectively.

The carbon content is expected to increase in weight percentage during carbonization and impregnation processes. The increasing pattern with increase in activation temperature from 500 to 800 °C may be due to an increasing of aromaticity of the carbon molecules. Consequently, hydrogen and nitrogen contents are decreased (Kumar & Jena, 2016).

However, the result does not relevant to indicate the suitability of the cocoa nibs as precursor for activated carbons. From various investigations on several agricultural by-products, the suitability for the production of high quality activated carbon is not determined from the composition of elements but by type-specific features (Gisi et al., 2016).

Table 3.4 Elemental analysis of cocoa nibs

Parameter	Element	Results (%)
1	Carbon	44.56
2	Hydrogen	7.20
3	Nitrogen	4.23
4	Sulphur	0.26

Table 3.5 shows the result of heavy metals determination in cocoa nibs using ICP-MS. The content of lead (Pb) was measured at fairly high concentration (1.096 ppm). The value of arsenic (As) and cadmium (Cd) were relatively low (0.172 and 0.717 ppm, respectively) while mercury (Hg) was not detected.

In the Fourteenth Schedule of Regulation 38, in the Malaysian Food Regulation 1985 from the Food Act 1983 states that the maximum permitted value of metal contaminants in cocoa and cocoa product such as As, Pb, Hg and Cd are allow to be present in less than 1.0, 2.0, 0.05 and 1.0 ppm, respectively (MOH, 2016). In

accordance, the quality index of activated carbon proposed by United State Pharmacopoeia (USP) outlines that the standard value for heavy metals must not exceed 0.005 of weight percentage (Wu et al., 2013).

The presence of heavy metals in cocoa nibs would be due to the growth factor where the chain of soil-plant-cocoa fruits took place (Wuana & Okieimen, 2011). Other factors that may affect the lead contamination are (i) fermentation and sun-drying process at cocoa farms and (ii) in between the shipping procedure (Rankin et al., 2005). It should be noted, that the study did not take into account the possibility of water used as a contributor of the metals (Onianwa et al., 1999). Overall, the study shows that the levels of the four heavy metals studied are generally within safe limits.

Table 3.5 Level of heavy metals in cocoa nib using ICP-MS

Sample Name	Dilution	As (ppm)	Cd (ppm)	Hg (ppm)	Pb (ppm)
Activated Carbon	500	0.172	0.718	<0.001	1.096

3.4.2 Characterization of the Prepared Activated Carbon

3.4.2.1 Surface Area and Porosity

Table 3.6 shows the surface area and porosity of the prepared activated carbon. The BET surface areas were found to be relatively high and comparable to the works reported in literatures (Liu et al., 2010, Njoku & Hameed, 2011, Yakout & El-Deen, 2016). The activated carbons prepared were found to have BET surface area which was as low as 190 m^2/g when pyrolysis at 500 °C and as high as 1313 m^2/g when activated at 800 °C. The total pore volumes measured were higher (1.2-1.9 cm^3/g) compared to commercially available activated carbon C1 (0.9 cm^3/g) and C2 (0.5 cm^3/g).

Cocoa nib's carbon which was impregnated with K_2CO_3 in specific activating agent to char ratio (1:1, 2:1 and 3:1) and was activated at 800 °C (named CNAC-800-1, CNAC-800-2 and CNAC-800-3, respectively) produced higher BET surface area (1,150, 1,244 and 1,313 m^2/g, respectively). The surface area of these activated carbons were significantly equivalent with two commercial activated carbons (C1 was 1,854 m^2/g and C2 was 1003 m^2/g).

Table 3.6 Surface area and pore characteristics of the prepared activated carbons

Sample ('prepared AC'-'activation temp'-'impregnation ratio')	BET Surface Area (m^2/g)	Micropore Surface Area (m^2/g)	Total Pore Volume (cm^3/g)	Micropore Volume (%)	Median Pore Width (nm)
CNAC-500-1	253.96	76.225	1.30	30.01	1.97
CNAC-500-2	329.89	120.38	1.44	36.49	1.99
CNAC-500-3	457.12	218.77	1.57	47.85	2.01
CNAC-600-1	756. 92	571.97	1.34	75.56	1.99
CNAC-600-2	999.13	796.14	1.36	79.68	1.99
CNAC-600-3	1,018.2	743.51	1.51	73.02	2.01
CNAC-700-1	459.61	53.202	1.20	11.57	4.75
CNAC-700-2	915.50	496.48	1.34	46.29	4.89
CNAC-700-3	1,103.0	727.55	1.23	65.96	4.90
CNAC-800-1	1,105.2	543.69	1.87	49.19	3.89
CNAC-800-2	1,200.8	692.08	1.93	57.63	3.78
CNAC-800-3	1,313.9	1,019.4	1.62	77.58	3.86
C1	1,854.9	1,608.8	1.55	86.73	1.83
C2	1,003.5	963.67	1.14	96.03	1.64
[1]Corncob	1273.91	n.a	0.90	n.a	3.03
[2]Bamboo	1432.00	n.a	0.70	n.a	n.a
[3]Olive stones	1218.00	n.a	0.60	n.a	n.a

C1-commercial activated carbon 1, C2-commercial activated carbon 2
[1]Njoku & Hameed, 2011
[2]Liu et al., 2010
[3]Yakout & El-Deen, 2016

Other BET surface area measured from agricultural waste-based activated carbons was 1,432 m^2/g from bamboo (Liu et al., 2010), 1,273 m^2/g from corncob (Njoku & Hameed, 2011) and 1,218 m^2/g from olive stones (Yakout & El-Deen, 2016). Liu et al. (2010), Njoku & Hameed, (2011) and Yakout & El-Deen, (2016) prepared the activated carbon using the chemical activation method.

Alias et al. (2017) had evaluated the effectiveness of K_2CO_3 in producing the activated carbon with higher number in surface areas and total pore volumes. They suggested that the development of porous structure of the activated carbons by K_2CO_3 activation is associated with gasification reaction, where K_2CO_3 accelerated the gasification process. During the heat treatment, the reduction of the potassium and the micro structural changes took place (Kamali & Fray, 2013).

Biomass such as cocoa nibs and other agricultural by-products formed of cellulose, lignin, and hemicellulose (natural polymer). During carbonization at high temperatures, the polymeric structures decompose and release most of the non-carbon elements mostly hydrogen, oxygen, nitrogen and minerals in the form of liquid (called as tars) and gasses. The carbons which are left behind formed a rigid carbon skeleton (Prahas et al., 2008).

In cellulosic materials, the carbonization temperature was found to be a crucial factor in developing a highly porous carbon structure. According to Fałtynowicz et al. (2015), thermal decomposition began at 50 – 200 °C where it associated with moisture release. Then, between 225 – 375 °C was where the most intensive decomposition of organic matter occurred. The celluloses and hemicelluloses underwent decomposition and released the volatile contents. When the temperature increased, the decomposition rate decreased and minimum weight loss occurred. This was due to formation of char structural units which was more resistant to thermal decomposition. However,

decomposition of higher thermal stability compounds took place, such as lignin. A total weight loss of approximately 74 % was recorded when the temperature reach 900 °C.

By referring to Table 3.11, a relatively similar phenomenon can be observed during this study. At temperature 500 °C and impregnated with K_2CO_3 at ratio of 1:1, the BET surface area was only developed at 253 m^2/g indicating the lesser formation of pores. From this figure (253 m2/g), 76 m^2/g was calculated as microporous surface area. However, when IR was increased (2:1 and 3:1), the surface area was increased too (329 m^2/g and 457 m^2/g, respectively). The microporous surface areas were also increased to 120 m^2/g and 218 m^2/g, respectively.

Additionally, as the temperature raised from 500 °C to 800 °C, both surface areas were increased gradually. Eventually, the activated carbon prepared at 800 °C with the IR of 3:1 was observed to have 1,313.88 m^2/g of BET surface area and 1,019 m^2/g of micropore surface area. Micropore volumes were increased from 30 % to almost 78 % of the pore volume. Median pore width was also increased from 1.97 nm (500 °C) to 3.86 nm (800 °C).

The results show the effect of carbonization temperatures and impregnation ratios to the BET surface area, mesopore surface area, pore diameter and total pore volume. Relatively similar results were observed by Okman et al. (2014) when they determined the surface area and porosity of the grape seed-based activated carbon which was impregnated with K_2CO_3 too. The activated carbon have 1,166 m^2/g BET surface area, 1,156 m^2/g of micropore surface area, 99.16 % of micropore volume and 1.6 nm of pore diameter resulted in a highly microporous activated carbon.

K_2CO_3 plays an important role in porosity development at different stages. When K_2CO_3 introduced to the precursor during the impregnation process, the partial structure of cocoa nibs was destroyed. K_2CO_3 altered the carbonization behavior of

cocoa nib, converted the contained minerals into soluble salts and established skeletal pore structure at the pre-carbonization period. Then, K_2CO_3 developed micropores abundantly and reduced the formation of graphitized carbon during the activation phase (Zhang et al., 2016).

It can be clearly observed from Table 3.11 the irregularities in the formation of pores which can be translated into the increasing or decreasing of surface area of the prepared activated carbon. When the char was activated at 700 °C and impregnated with ratio of 1:1, the BET surface area calculated was only 459 m^2/g with 53 m^2/g of micropore surface area. It showed a relatively high decreased in surface area compared with the previous activated carbon prepared at 600 °C and impregnated with ratio of 3:1 (1,018 m^2/g of BET surface area and 743 m^2/g of micropore surface area). This was an indication of a structural collapse in the carbon structures. However, the surface area was gradually increased as impregnation ratio was increased (from 1:1 to 3:1). It showed the influence of K_2CO_3 in development of new pores and improvement of miroporous structures in the carbon.

Figure 3.2 shows a plotted graph for the pore size distributions of cocoa nib-based activated carbon, based on these data. As can be seen from this plot, singular sharp peaks were detected in the range of 20 to 40 Angstrom (Å) (or 2 to 4 nm).

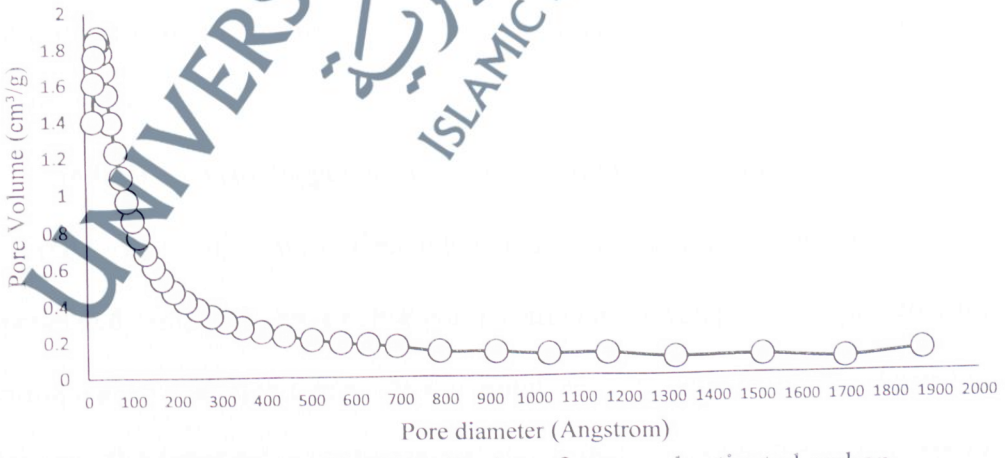

Figure 3.2 Pore Size Distribution of prepared activated carbon.

About 73 % of the pores had their diameter within the mesopores range (pore diameter range of 20–500 Å). Hence, the cocoa nib-based activated carbon is mesoporous material. This suggests the prepared activated carbon would be very absorptive to aqueous sample.

Carbonization in inert condition could yield a mesopore carbon of a very narrow pore size distribution. Carbon with narrow pore size distributions is stable in structure that could improve practical parameters such as BET surface area and V_0 total micropore volume (Łukaszewicz & Zieliński, 2011).

3.4.2.2 Surface Morphology

Figure 3.3 (a) shows the SEM micrographs of the cocoa nib's char under 10000x magnification while (b) is the micrographs of the activated carbon under 10000x magnifications. Both micrographs presented with the morphological changes of the carbon materials during carbonization and activation processes.

After carbonization was performed under inert condition, some irregular holes and pores were developed on the surfaces of the chars as can be observed in Figure 3.3 (a). This was due to the sudden burst of the thermal expansion from pyrolysis. Pore development in the char during pyrolysis was important as it would increase the surface area and pore volume of the activated carbon after the activation process (Ahmad & Alrozi, 2010).

In figure 3.3 (b), bigger heterogeneous and irregular shape pore structures were observed. More pores were developed and were closed to each other. K_2CO_3-impregnated sample shows a better porous structure development compared with the non-impregnated sample (char). At this point, the porous structure has been formed where exterior pores serve as the main channels that connect to the inner pores of the

carbon. However the structure has been partly broken where the surface was eroded during the activation process where similar observation was obtained by (Hao & Xianlun, 2013).

The introduction of K_2CO_3 enlarged the difference between the morphology on the surface of the char and of the activated carbon. The reactions between K_2CO_3-carbon took place due to the diffusion effect and the heat was transferred into the molecules which create more pores in the activated carbon (Tan et al., 2008). Okman et al. (2014) observed a spongy-like structures with many small cavities in the grape seed-based activated carbon which was impregnated with K_2CO_3.

It can be observed in Figure 3.3 (b) the presence of small white particles of various sizes attached to the surface of the activated carbon. The white particles were believed to be the residues of potassium salt (from K_2CO_3) where a similar finding was observed by Mopoung (2008) while preparing the banana peel-based activated carbon. This indicates that the traces of potassium salts residues are present in the carbon matrix even though intensive washing procedure with the combination of HCl and boiled-H_2O was applied.

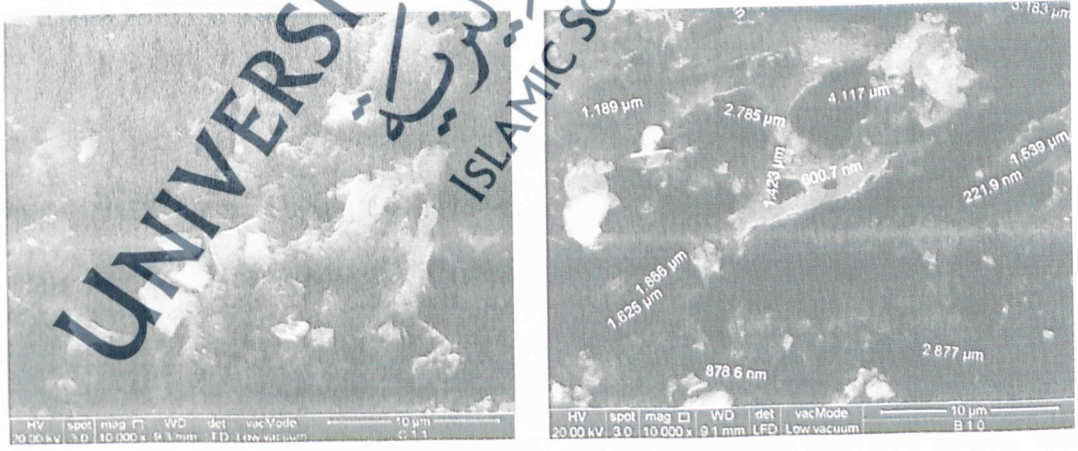

(a) (b)

Figure 3.3 (a) SEM micrograph of cocoa nibs char and (b) prepared activated carbon.

3.4.2.3 Surface Functional Groups

Figure 3.4 exhibits the similarities in the pattern of the FTIR spectrum for the cocoa nib char, cocoa nib-based activated carbon and commercial activated carbons (C1 and C2). Table 3.7 lists the wavenumbers of FTIR spectrum detected in the carbon.

It can be observed that in infrared spectrum for the prepared activated carbon, peaks were detected at 2324 (C≡N), 2115 (C≡C), 1990 and 1837 (combination bands of aromatic hydrocarbon), 1793 (C=O of carboxylic group) and 1570 cm^{-1} (C–C of aromatic hydrocarbon). A relatively similar pattern of the FTIR spectrum demonstrated by the cocoa nib-based activated carbon was observed on the commercial activated carbons (C1 and C2). This indicates that the surface functional groups on the cocoa nib-based activated carbon are relatively similar to the commercial activated carbons.

Figure 3.4 FTIR spectrums for the prepared and commercial activated carbons.

Oxygen functional groups (C=O) was detected in the prepared activated carbon. The presence of oxygen functional group on the surface of activated carbon was expected to indicate the polarity. Oxygen functional group was expected to bind water

and to facilitate the formation of water clusters. The presence of C=O in aromatic groups exhibited strong oxygen functional group intensity, which indicates hydrophilic characteristics (Ahmad et al., 2013).

The prepared activated carbon was also showed significant formation of nitrile groups (C≡N). The introduction of nitriles increased the basicity of the carbon. This was due to the isolated electron in the nitrogen atom (Ahmad et al., 2013).

Table 3.7 Infrared assignment of functional groups on the prepared activated carbon surface (Adapted from Ahmad et al., 2013).

Characteristics	Wave numbers range (cm^{-1})	Prepared Activated Carbon
Aliphatic Hydrocarbons		
C-H	3100 – 2850	Not detected
C=C	> 3000	Not detected
C≡C	2260 - 2100	2315
Aromatic Hydrocarbons		
C-H (out of plane)	< 900	Not detected
C=C	1620 – 1400	1570
Combination bands	1900 – 1700	1990, 1837
Oxygen functional groups		
C-O	1300 – 1080	Not detected
C=O	1760 – 1690	1793
O-H	3600 - 3200	Not detected
Nitrogen functional groups		
C≡N	2400 – 2300	2323

3.4.3 Characterization of the Demineralized Activated Carbon

Due to its characteristics, the activated carbon prepared at 800 °C with impregnated ratio of 3:1 (CNAC-800-3) was selected to undergone the demineralization process. The acid treated activated carbon was named CNAC-D3.

3.4.3.1 Adsorption Isotherm

Figure 3.5 shows the adsorption isotherms of CNAC-800-3 and CNAC-D3. The different shapes of the adsorption isotherm are a reflection of the different pore size distribution in the activated carbon samples.

It can be observed that the isotherms of CNAC-800-3 and CNAC-D3 resembled a combination of types II and I with prominent hysteresis loops of type H4 (according to IUPAC classification of hysteresis loops), which occur in the region of 0.2 to 0.8 P/P_o. This shows the higher degree of mesoporosity contained in both carbons (Mak et al., 2009).

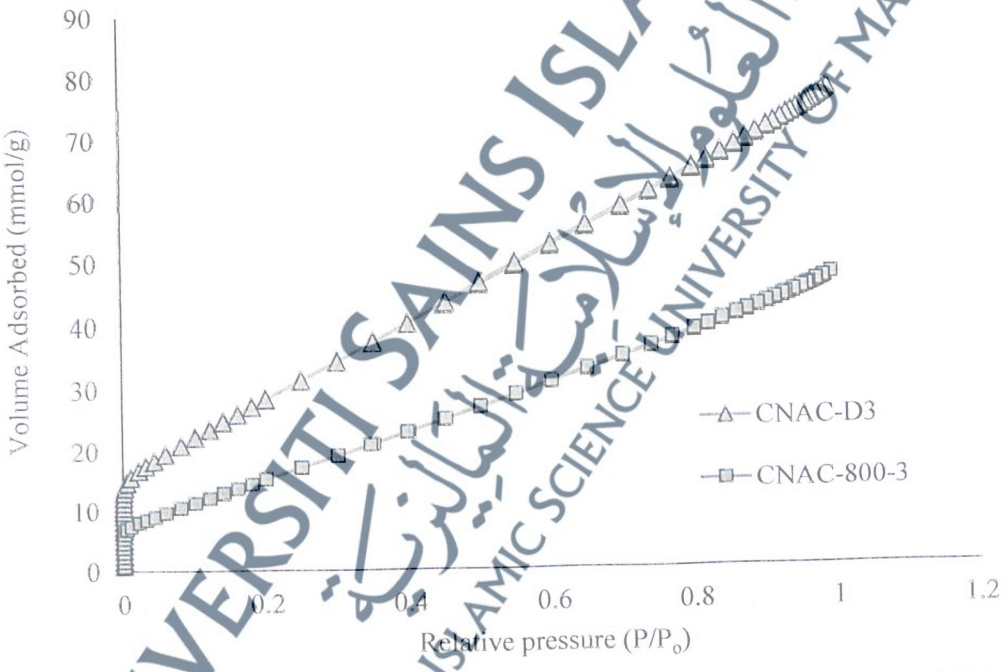

Figure 3.5 Adsorption isotherm of CNAC-800-3 and HCl treated CNAC-D3.

Both carbons showed a less steep Type I isotherm with a sharp "knee" form at the low relative pressure and a gradual increase in nitrogen gas (N_2) uptake at the higher pressure. The gradual increase in N_2 uptake occurred beyond $P/P_o > 0.2$, thus showing

the heterogeneous microporosity and growth of small size mesoporosity (Nakagawa et al., 2007).

HCl treatment increased the adsorbed amount of nitrogen for CNAC-D3 in the region of 0 to 1 P/P_o. Both isotherms presented with a steep adsorption at very low relative pressures (P/P_o = 0 to 0.2) characteristic of microporous structures (Nakagawa et al., 2007). The hysteresis loop type H4 characterized the presence of mesopores particles. CNAC-D3 showed the higher adsorption and CNAC-800-3 showed the lowest adsorption of the series in the low-pressure region. HCl treatment increased the amount adsorbed at low relative pressures.

CNAC-D3 adsorbed almost twice more N_2 than CNAC-800-3, which indicate a higher surface area. The sloped-up plateau started at $P/P_o > 0.2$. The increase in N_2 uptake at the other pressures showed the increase of micropore diameter and growth of mesoporosity (Nakagawa et. al., 2007).

3.4.3.2 Surface Area and Pore Developments

Table 3.8 shows the pore characteristics of cocoa nib-based activated carbon before and after acid treatment. These data show the treatment process has resulted in an increase in both the surface area and pore volume. The effects of the treatment change the ash content, pore structure, surface functionality and adsorption capacity (Bhatnagar et al., 2013).

The comparison was made between CNAC-800-3 and CNAC-D3. From the table, it can be observed that the surface areas for the prepared activated carbons were increased after the hydrochloric acid treatments. The surface area for CNAC-800-3 had increased from 1,313.9 to 1,932.4 m^2/g (86 % increases) in CNAC-D3.

Table 3.8 The surface area of cocoa nib-based activated carbon before and after acid treatment

Sample ('prepared AC'-'activation temp'-'impregnation ratio')	BET Surface Area (m^2/g)	Micropore Surface Area (m^2/g)	Total Pore Volume (cm^3/g)	Micropore Volume (%)	Median Pore Width (nm)
Prepared Activated Carbon					
CNAC-800-3	1,313.9	1,019.4	1.62	77.61	3.86
Prepared Activated Carbon Treated With HCl					
CNAC-D-3	1,932.4	1,272.6	2.67	65.83	3.45

The total pore volumes were observed to increase in CNAC-800-3 after the acid treatments (1.62 cm^3/g to 2.67 cm^3/g) with 64 % increment. Although the micropore volume was recorded to decrease in CNAC-D3 compared with CNAC-800-3, the micropore surface area was increased from 1,019 m^2/g to 1,276 m^2/g (25 % increment). The volume reduction was about 11 %. The pore size of CNAC-800-3 was decreased from 3.86 nm to 3.45 nm, with 10 % of pore size reduction.

The patterns of microporosity in both untreated and treated activated carbons can be determined with the micropore surface area. It was clearly understood from the table that the demineralized activated carbons have more microporous structures compared with the untreated activated carbons. Although the percentage of micropore volume in CNAC-D3 was smaller than CNAC-800-3, the micropore surface area in CNAC-D3 was higher compared with CNAC-800-3 (increased in 24 %).

Carbonization at 500 °C can develop basic microstructure of porosity. The developed pores are prone to be filled with tarry products which produced during pyrolysis. The higher temperature of carbonization assists the removal of tarry and disorganised matter, hence eliminating constrictions and forming a more accessible pore structure (Illingworth et al., 2013).

Besides tarry products, mineral oxides were also present in ash matrix which usually blocked the pores structures. However, with the acid treatment, some of the minerals are leached out from the structure and increase the surface area and carbon porosity (Shawabkeh et al., 2015).

HCl treatment increased the adsorbed amount of N_2 for CNAC-D3 in the region of 0 to 1 P/P_o. In both activated carbons, the isotherms developed were a steep adsorption at very low relative pressures (P/P_o = 0 to 0.2) characteristic of microporous structures. The hysteresis loop type H4 characterizes the presence of mesopores particles. CNAC-D3 presents the higher adsorption and CNAC-800-3 presents the lowest adsorption of the series in the low-pressure region. Therefore, HCl treatment was proven to increase the surface area and porosity of cocoa nib-based activated carbon.

The development of more surface area and pores in activated carbon treated with HCl solution is likely to be due to the elimination of impurities on the surface and/or in the pores. Activated carbon can consist of mineral matter up to 15 % in the form of ash content, which clogs up in the pores (Aji et al., 2015).

According to Nuithitikul (2010), the minerals are regarded as unwanted contaminants such as N, P, Si, Ca, Na, K, Al, Zn and Fe. In order to purify the prepared activated carbon and to remove the contaminants, acid solution is usually used during washing part and in further treatment. These inorganic elements could be removed from activated carbon with HCl, H_2SO_4 or HF treatment in order to reduce the ash content.

Table 3.9 demonstrates the effect of HCl treatment to the ash content of the prepared activated carbon. It can be observed that the ash content of CNAC-D3 has been decreased to more than half, contrasting to that of CNAC-800-3. In addition, commercial activated carbons contained relatively higher ash content compared with

the prepared and the treated activated carbon. Therefore, HCl treatment was proven effective to be used in eliminating the ash content from the activated carbon.

Table 3.9 The ash content in HCl treated and untreated activated carbons

Untreated activated carbon		Treated activated carbon	
Sample	Ash content (%)	Sample	Ash content (%)
CNAC-800-3	15.52	CNAC-D3	3.26
C1	11.11		
C2	23.81		

3.4.3.3 Surface Morphology

Figure 3.6 shows the SEM micrograph image of CNAC-D3. The activated carbon formed irregular, large caved-in shaped cavities on its surface. The smallest pore developed onto CNAC-D3 was sized of 0.4317 µm and the largest was 4.802 µm. Whereas the largest pore developed onto the surface of untreated activated carbon was 4.117 µm (Figure 3.3 (b)).

The micrograph image showed the development of more porous structure in CNAC-D3, compared with CNAC-800-3 (Figure 3.3 (b)). The acid treatment was proven to affect the morphology and structure of the activated carbon. This means that during carbonization, the organic compounds together with carbon were forced to leave the structure, and pores were created. However, minerals were left in the pores. The application of hydrochloric acid solutions on the activated carbon resulted in the elimination of these inorganic components, which was similarly reported by Nuithhitikul et al. (2009) and Bhatnagar et al. (2013).

Figure 3.6 SEM micrograph shows larger pore size developed on CNAC-D3.

3.4.3.4 Surface Chemistry

Figure 3.7 shows the spectrums of the activated carbon samples (CNAC-800-3 and CNAC-D3). Both activated carbons developed a relatively similar spectrum and exhibit relatively similar peaks. There is no reduction of peaks in both spectrums between 3500 and 800 cm^{-1} except for band 1570 cm^{-1} (very weak) in CNAC-800-3, which was disappeared in CNAC-D3. This indicates that the acid treatment was not significant in altering the surface functional groups in CNAC-800-3, as CNAC-800-3 was already washed extensively with a combination of hot water and hydrochloric acid in order to remove the remaining K_2CO_3 after activation process.

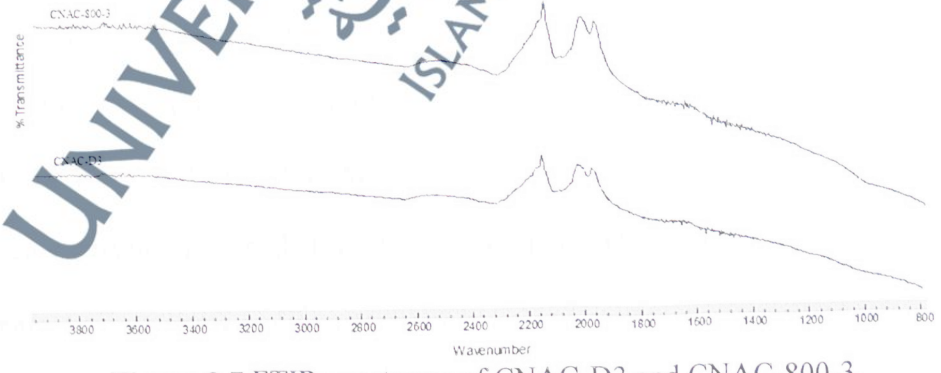

Figure 3.7 FTIR spectrums of CNAC-D3 and CNAC-800-3.

3.4.3.5 Principal Component Analysis

Principal component analysis (PCA) was used to any similarities or differences between the commercial activated carbons (C1 and C2) and the prepared activated carbons (CNAC-500-1, 500-2, 500-3, 600-1, 600-2, 600-3, 700-1, 700-2, 700-3, 800-1, 800-2 and CNAC-800-3) in terms of their physical and chemical properties. CNAC-500-1, CNAC-500-2 and CNAC-500-3 were the activated carbons that were prepared at carbonization temperature of 500 °C and were impregnated with K_2CO_3 at ratio of 1:1, 1:2 and 1:3, respectively. CNAC-600-1, CNAC-600-2 and CNAC-600-3 were prepared at 600 °C of the carbonization temperature and the impregnation ratio was followed the sequence from the previous groups. CNAC-700-1, CNAC-700-2 and CNAC-700-3 were prepared at 700 °C and CNAC-800-1, CNAC-800-2 and CNAC-800-3 were prepared at 800 °C. CNAC-D1, CNAC-D2 and CNAC-D3 were the hydrochloric acid treated activated carbons of CNAC-800-1, CNAC-800-2 and CNAC-800-3.

The commercial activated carbon was NORIT activated charcoal (C1) and Ultracarbon Medicinal Charcoal (C2) produced by Merck KGaA. The similarity among the activated carbons will be shown in the scores plot where the carbon located in the same cluster or group. The scores plot provides a visualization of the relationship between the prepared activated carbons and commercial activated carbons.

Prior analysis, all the prepared activated carbons were coded as AC1, AC2, AC3, AC4, AC5, AC6, AC7, AC8, AC9, AC10, AC11 and AC12. The acid treated activated carbon were coded as AC13, AC14, AC15 and the commercial activated carbons were coded as AC-C1 and AC-C2.

Table 3.10 represents the raw data of the prepared activated carbons and the commercial activated carbons which were selected as the parameters for PCA. The data

matrix was in dimension 17 x 11, where 17 is the number of activated carbons and 11 is the number of variables. The parameters related to physical and chemical properties of the carbon are BET surface area, BJH volume, BET diameter (pore size) and wave numbers for surface functional groups.

Table 3.10 Cleaned data matrix with maximum normalization of prepared and commercial activated carbons

	S_{BET}	V_{BJH}	D_{BET}	Peak 1	Peak 2	Peak 3	Peak 4	Peak 5	Peak 6	Peak 7	Peak 8
AC1	0.0718	0.0005	0.0103	0.0000	0.6724	0.7513	0.7876	0.7977	0.0000	0.8757	1.0000
AC2	0.0915	0.0005	0.0089	0.3677	0.6700	0.7499	0.0000	0.7948	0.0000	0.8732	1.0000
AC3	0.1393	0.0005	0.0064	0.3714	0.6718	0.0000	0.7862	0.7954	0.0000	0.8754	1.0000
AC4	0.1256	0.0005	0.0063	0.0000	0.6781	0.7481	0.7865	0.7952	0.0000	0.8745	1.0000
AC5	0.1500	0.0005	0.0067	0.0000	0.7675	0.8558	0.9001	0.9098	0.0000	1.0000	0.0000
AC6	0.1615	0.0005	0.0053	0.0000	0.7002	0.7541	0.7928	0.7986	0.8668	0.9024	1.0000
AC7	0.2380	0.0004	0.0029	0.0000	0.6707	0.7499	0.7897	0.7959	0.8685	0.8992	1.0000
AC8	0.3056	0.0004	0.0025	0.0000	0.6709	0.7497	0.7850	0.7949	0.0000	0.8733	1.0000
AC9	0.3670	0.0004	0.0019	0.0000	0.6708	0.7517	0.7869	0.7950	0.0000	0.8749	1.0000
AC10	0.4329	0.0007	0.0024	0.0000	0.6418	0.7516	0.7853	0.7977	0.0000	0.8745	1.0000
AC11	0.5356	0.0009	0.0027	0.0000	0.7563	0.8562	0.8977	0.9050	0.0000	1.0000	0.0000
AC12	0.4947	0.0006	0.0019	0.0000	0.6631	0.7519	0.7870	0.7965	0.0000	0.8750	1.0000
AC13	0.5966	0.0010	0.0024	0.0000	0.6370	0.7509	0.7876	0.7967	0.0000	0.8765	1.0000
AC14	0.6862	0.0006	0.0016	0.0000	0.6626	0.7502	0.7839	0.7952	0.0000	0.8740	1.0000
AC15	0.9226	0.0008	0.0016	0.0000	0.6432	0.7494	0.7864	0.7965	0.0000	0.8756	1.0000
AC-C1	0.7996	0.0003	0.0011	0.3720	0.6701	0.7512	0.7860	0.7960	0.0000	0.8748	1.0000
AC-C2	0.6437	0.0002	0.0000	0.0000	0.6265	0.7488	0.7862	0.7955	0.0000	0.8750	1.0000

Among the prepared activated carbons, AC15 showed a relatively similar surface area (1932 m^2/g) to that of AC-C1 (1854 m^2/g), and better than AC-C2 (1003 m^2/g). Prior analysis with PCA, the raw data was preprocessed using maximum normalization. Normalization is essential because PCA is an exercise of maximize the variance. By this practice, it will improve the accurateness and the usefulness of the parameters (Dinç et al., 2014).

The first observation was made on the correlation of the activated carbons with the FTIR peaks of functional groups. The prepared activated carbons (AC1, AC2, AC3, AC4, AC5, AC6, AC7, AC8, AC9, AC10, AC11, AC12, AC13, AC14 and AC15) and the commercial activated carbons (AC-C1 and AC-C2) were studied against the FTIR peaks (peak 1, 2, 3, 4, 5, 6, 7 and 8). Figure 3.8 shows the Scores Plot while Figure 3.9 shows the Loadings Plot.

The Scores Plot displayed the location of the samples AC1, AC2, AC3, AC4, AC6, AC7, AC8, AC9, AC10, AC12, AC13, AC14, AC15, AC-C1 and AC-C2 at the positive side of PC-1. The location of AC5 and AC11 were at far end of negative side on PC-1 (not shown in the graph). The plot showed that AC6 and AC7 were on the positive side of PC-2 while the other samples were on the negative side.

It can be observed that there were three groups of data in the plot. AC6 and AC7 were in the first group while AC1, AC4, AC8, AC9, AC10, AC12, AC13, AC14, AC15 and AC-C2 were in the second group. AC2 and AC3 were considered to be in the third group while AC-C1 was place alone between the second and third group.

By referring to Table 3.10, the plot pattern suited the developed data. For example, peak 1 was only obtained in AC2, AC3 and AC-C1 and peak 6 was found only in AC6 and AC7. Other activated carbons (AC1, AC4, AC8, AC9, AC10, AC12, AC13, AC14, AC15 and AC-C2) were having relatively similar peaks.

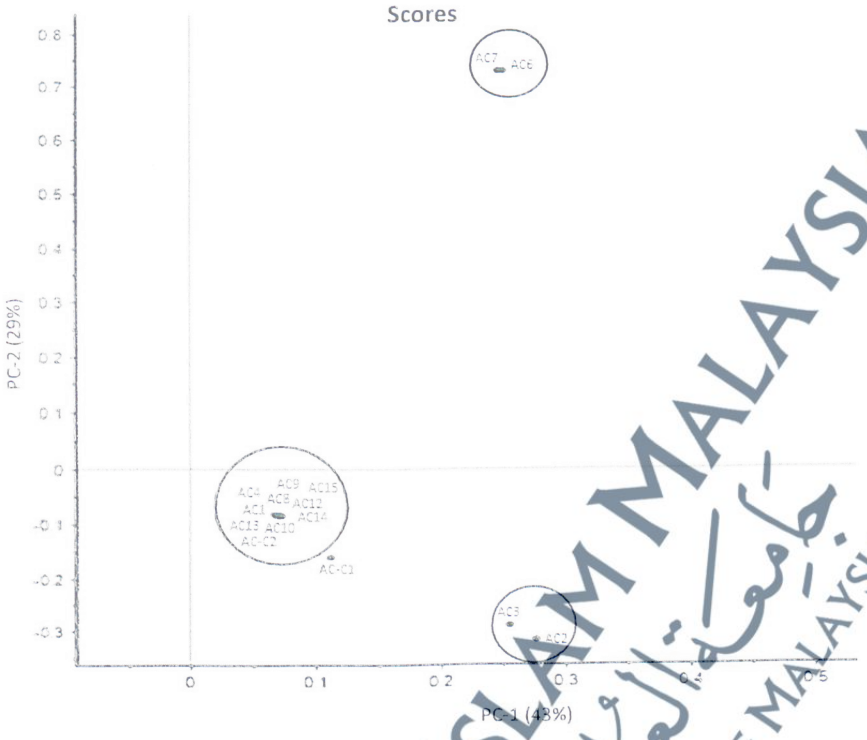

Figure 3.8 Scores Plot of PC-2 vs PC-1.

Figure 3.9 shows a Loadings Plot of PC-2 vs PC-1. The plot showed that peak 2, peak 3, peak 4, peak 5 and peak 7 were anti-correlated with positive values for PC-1 (peak 1, peak 6 and peak 8). It can be observed too that peak 1 and peak 8 were at the negative side of PC-2 and peak 6 was at the top of positive side of PC-2.

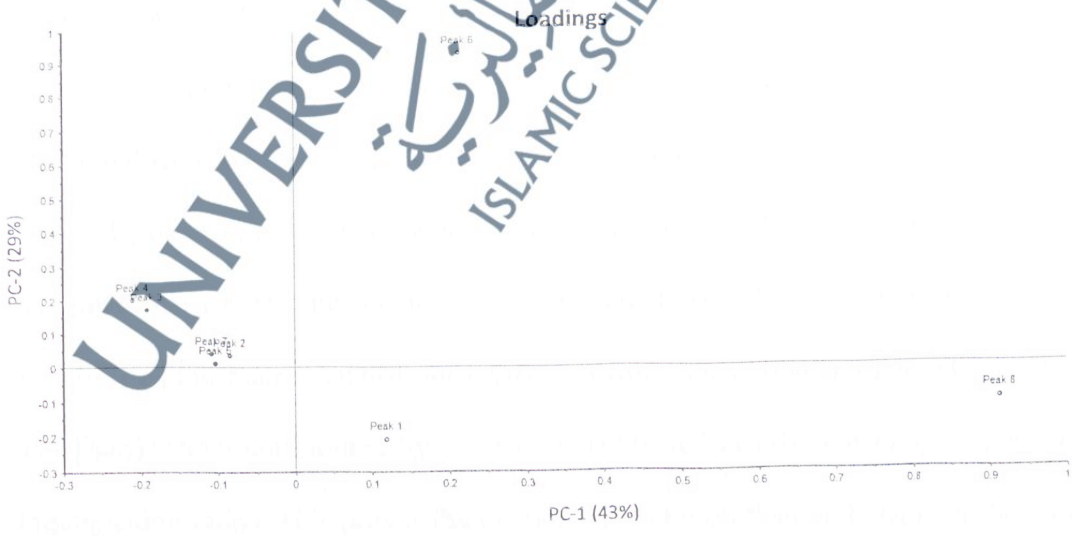

Figure 3.9 Loadings Plot of PC-2 and PC-1.

In the second analysis, the activated carbons were tested against the porosity characteristics which consist of BET surface area (S_{BET}), BJH volume (V_{BJH}) and BET pore diameter (D_{BET}). Figure 3.10 shows the Scores Plot of the analysis while Figure 3.11 shows the Loadings Plot. From Figure 3.10, it can be observed that the graph showed the difference among the activated carbons which can be divided into five groups.

AC1 and AC2 were witnessed to have been located at the lowest negative side of PC-2 and PC-1; and can be considered as the first group. AC3 and AC5 together with AC4 and AC6 can be considered as the second group, which were located at the negative side of PC-1. However, AC3 and AC5 were placed at negative side of PC-2 while AC4 and AC6 were at the positive side. AC7 to AC9 were at the positive side of PC-2 but at the negative side of PC-1 and were considered as the third group. AC10, AC12 and AC-C2 were the fourth group which located at the positive side of PC-1 and PC-2. AC11, AC13, AC14, AC-C1 and AC15 were grouped together as group five which laid at positive side of PC-1 but at negative side of PC-2.

From the plot, it can be seen that AC-C1 was located near to the position of AC14 and AC15. The position of AC-C2 was near to AC12 and AC14 but relatively far from AC-C1 and AC15. This observation was significant to show the similarity of AC15 and AC14 with AC-C1; and AC12 and AC14 with AC-C2.

Figure 3.11 displays a Loadings Plot of the above analysis. The plot showed that V_{BJH} and D_{BET} were located on the center of the graph while S_{BET} was at the top positive side of the plot. S_{BET} is significantly different from others porosity parameters (V_{BJH} and D_{BET}) which contributed by surface areas created at different temperatures and impregnation ratios. This proves the relationship between S_{BET} and D_{BET}, as shown in Table 3.10 where the D_{BET} decreased when S_{BET} increased.

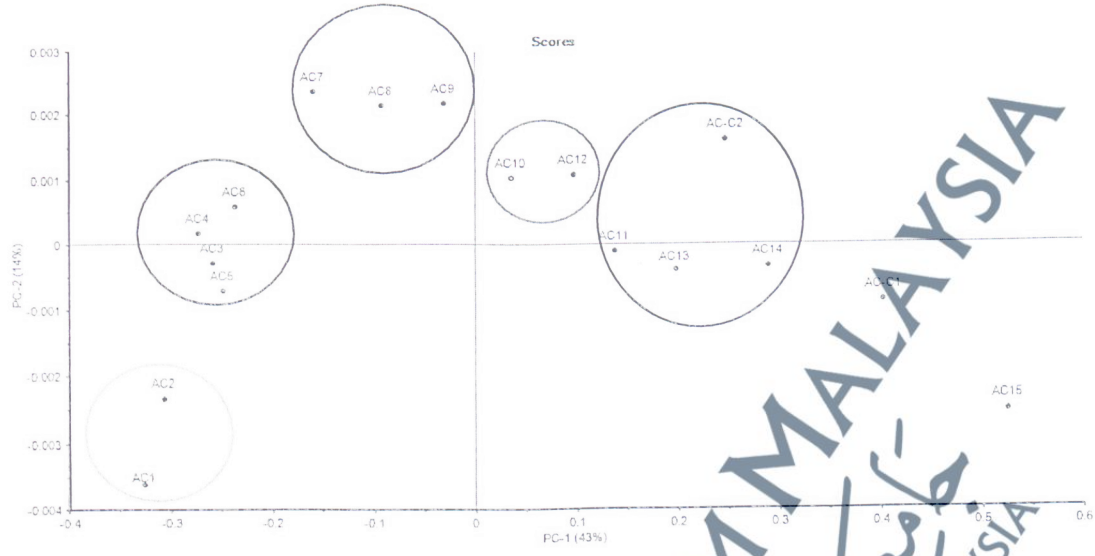

Figure 3.10 Scores Plot of PC-2 vs PC-1.

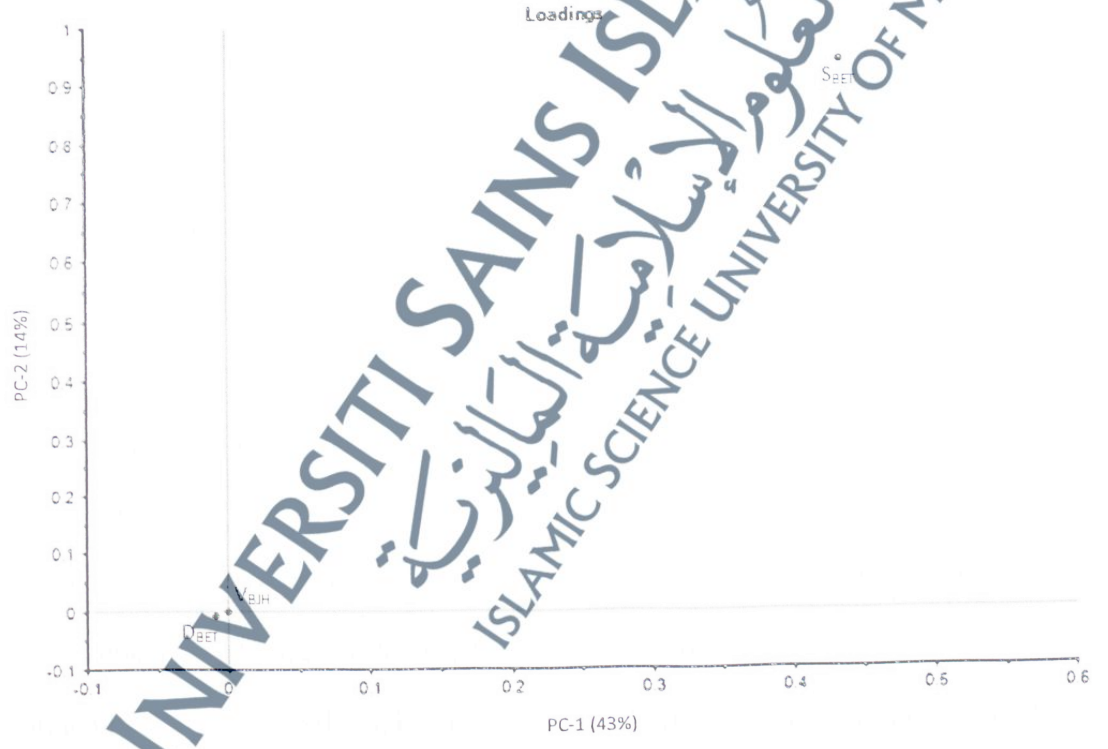

Figure 3.11 Loadings Plot of PC-2 and PC-1.

The objectives of the experiment are to evaluate the prepared activated carbons according to the structures (porosity) and the surface functional groups. In the first analysis, most of the prepared activated carbons were relatively similar with AC-C2;

and only AC2 and AC3 were having similarity with AC-C1. In the second analysis, AC15 and AC14 were relatively similar with AC-C1 and AC12 and AC14 were fairly comparable with AC-C2. Therefore, it can be evidently concluded that AC12, and AC14 were belong to the same group as AC-C2 and; AC15 and AC14 were in the same group as AC-C1.

AC-C1 and AC-C2 are popular among consumers in poisoning treatment. The findings can be used as an essential point to claim that the activated carbons prepared from cocoa nibs waste significantly have the potential to be used as a medicinal grade activated carbon.

3.5 Conclusion

This study showed that the use of K_2CO_3 as activating agent along with the two-step pyrolysis under inert condition, played an important role in preparing and changing cocoa nibs into well-developed porosity activated carbon. It generated mostly microporous carbon in which the percentage of micropore was between 75 % and 80 % and the average pore diameter of 5 nm. However, the prepared activated carbon contained deposited of K_2CO_3 and inorganic constituents on the surface and/or in the pores. Intensive washing process had driven off some of these deposits to improve porosity. The HCl treatment on the prepared activated carbon managed to eliminate the remaining minerals and developed a highly porous carbon structure. Using multivariate principle component analysis, it was proven that the de-ash activated carbon (AC14 and AC15) was having a relatively similar characteristics of that commercial activated carbons (AC-C1 and AC-C2). These data proved that cocoa nibs waste has potential as a precursor in preparing a clean, cheap and highly efficient activated carbon.